Application of the density matrix renormalization group in momentum space

Satoshi Nishimoto, Eric Jeckelmann, and Florian Gebhard
Fachbereich Physik, Philipps–Universität Marburg, D-35032 Marburg, Germany

Reinhard M. Noack
Institut für Physik, Johannes-Gutenberg-Universität Mainz, D-55099 Mainz, Germany

(Received 19 October 2001; published 10 April 2002)

We investigate the application of the density matrix renormalization group (DMRG) to the Hubbard model in momentum space. We treat the one-dimensional models with dispersion relations corresponding to nearest-neighbor hopping and $1/r$ hopping and the two-dimensional model with isotropic nearest-neighbor hopping. By comparing with the exact solutions for both one-dimensional models and with exact diagonalization in two dimensions, we first investigate the convergence of the ground-state energy. We find variational convergence of the energy with the number of states kept for all models and parameter sets. In contrast to the real-space algorithm, the accuracy becomes rapidly worse with increasing interaction and is not significantly better at half filling. We compare the results for different dispersion relations at fixed interaction strength over bandwidth and find that extending the range of the hopping in one dimension has little effect, but that changing the dimensionality from one to two leads to lower accuracy at weak-to-moderate interaction strength. In the one-dimensional models at half filling, we also investigate the behavior of the single-particle gap, the dispersion of spinon excitations, and the momentum distribution function. For the single-particle gap, we find that proper extrapolation in the number of states kept is important. For the spinon dispersion, we find that good agreement with the exact forms can be achieved at weak coupling if the large momentum-dependent finite-size effects are taken into account for nearest-neighbor hopping. For the momentum distribution, we compare with various weak-coupling and strong-coupling approximations and discuss the importance of finite-size effects as well as the accuracy of the DMRG.

DOI: 10.1103/PhysRevB.65.165114 PACS number(s): 71.10.Fd, 71.27.+a

I. INTRODUCTION

Many renormalization schemes are carried out in momentum space and involve integrating out degrees of freedom using a momentum cutoff. For example, Wilson's[1] numerical renormalization group (RG) implements this program using a mapping of momentum shells to an effective lattice model. The renormalization process is carried out by successive numerical diagonalization of a finite system and energetic truncation of the Hilbert space. While this lattice model corresponds to successive momenta or, equivalently, energy scales, its form is similar to that of a strongly correlated lattice model.

Attempts at applying a real-space version of the Wilson procedure to short-range quantum lattice models such as the Heisenberg or the Hubbard model were not successful, however, because successive lattice points do not correspond to different energy scales. The density matrix renormalization group (DMRG) (Refs. 2 and 3) overcomes these limitations by carrying out the renormalization on a subsystem. The truncated basis is formed by projecting the state of the entire system onto the subsystem using the reduced density matrix rather than selecting states energetically. This method has been very successful at treating low-dimensional quantum lattice models with open boundary conditions and short-range couplings. However, for longer-range off-diagonal interactions, higher dimensional systems or lattices with periodic boundary conditions, this real-space formulation of the DMRG is much less successful. In addition, it loses sight of an energy- or momentum-based classification of the relevant degrees of freedom.

A potential way of overcoming this limitation for itinerant electron systems is to apply the DMRG ideas to the momentum-space formulation of the Hamiltonian. This approach has a number of potential advantages over the real-space approach. First, since the single-particle basis in momentum space is explicitly translationally invariant, momentum is a conserved quantum number. Use of this momentum quantum number reduces the size of the Hilbert space in the diagonalization. Second, momentum-dependent quantities such as the momentum distribution or the dispersion of excitations can be directly calculated. Third, the kinetic energy term is diagonal so that varying the dispersion by, for example, changing the range of the hopping, is easy to do.

Attempts to formulate a numerical renormalization group procedure for quantum lattice systems in momentum space[4] predating the DMRG were not particularly successful—this was one of White's motivations for turning to real space and formulating the DMRG. Shortly after the development of the DMRG in real space, White attempted to use DMRG methods on the momentum-space formulation of the Hubbard model. He calculated the ground-state energy in one and two dimensions at intermediate couplings, but found that the energies obtained were not significantly better than those obtained by other variational methods.[5]

Independently, Xiang developed a similar technique and applied it to the Hubbard model in one and two dimensions.[6] In this work, Xiang outlined an efficient implementation of the DMRG in momentum space. He developed a factorization of the Hubbard interaction that reduces the number of

 ©2002 The American Physical Society

terms from N^3, where N is the number of single-particle Bloch wave functions in the lattice, to $6N$. He also pointed out some features of the algorithm that need to be carefully considered in momentum space: Since the interaction is highly nonlocal, there is no natural ordering of the single-particle states; the choice of the ordering can, however, have an effect on the performance of the DMRG algorithm. In addition, there is no well-defined infinite-system algorithm, so that care must be taken in how the lattice is built up initially. Care must also be taken in this initialization procedure so that states with a sufficient spread in momentum quantum numbers are kept. One possible outcome of an inadequate initialization procedure is convergence to a state other than the true ground state.

Xiang investigated the performance of the algorithm for various interaction strengths for the one-dimensional Hubbard model with 16 sites at half filling, and for the two-dimensional model on system sizes ranging from 4×4 to 12×12 for various band fillings. He found that the convergence of the method depends strongly on the interaction strength, U. The method is exact for $U=0$ since the Hamiltonian is diagonal and the convergence becomes rapidly worse with increasing U. In one dimension, he compared with real-space DMRG calculations and found that the error in the ground-state energy was higher than the real-space calculation for both weak and intermediate interaction strengths ($U/t=1$ and 4, with t the hopping matrix element), with 5% error for $U/t=4$. In two dimensions, he compared with exact diagonalization for a 4×4 system, cluster diagonalization on a 6×6 system, and quantum Monte Carlo and stochastic diagonalization calculations on 4×4, 6×6, and 8×8 systems. The relative errors increased rapidly with U for the 4×4 system. The variational energies were comparable to those of the stochastic diagonalization and quantum Monte Carlo methods (for which the energy is nonvariational) for larger system sizes. The variational bounds for the energy were slightly higher than stochastic diagonalization for the 6×6 lattice and slightly lower for the 8×8 lattice. In comparing the performance in one and two dimensions, Xiang pointed out that the accuracy for given U/t, band filling, and number of states, kept for 16 site systems was better in two dimensions than in one, leading him to speculate that the momentum-space method becomes more accurate as the dimensionality is increased.

Our purpose in this work is to explore more fully both the convergence properties and the application of the momentum-space formulation of the DMRG to the Hubbard model. In one dimension, we take advantage of the existence of exact solutions for two choices of the dispersion, corresponding to nearest-neighbor hopping and $1/r$ hopping, to systematically investigate the dependence of the convergence of the ground-state energy on interaction strength, band filling, and the number of density-matrix eigenstates kept m. We investigate the regularity of the convergence with m and discuss schemes to extrapolate in m in order to obtain more accurate energies. We reexamine the relative convergence for the one- and two-dimensional models with a view to understanding the utility of the momentum-space DMRG for higher-dimensional systems.

While the ground-state energy is useful for determining variational convergence, it does not directly provide much useful information about the physical behavior of the system. We therefore investigate some physically useful quantities, the quasiparticle gap, the momentum distribution, and the dispersion of spinon excitations, for the one-dimensional models and compare to exactly known results and perturbative approximations, where appropriate. Our calculations of the momentum distribution and the spinon dispersion for the $1/r$-hopping model are, to our knowledge, the first independent numerical calculations of these quantities.

The layout of the remainder of this paper is as follows. In Sec. II we discuss the model systems and their basic properties. Our DMRG method is described in Sec. III. The convergence and accuracy of the momentum-space DMRG are discussed in Sec. IV. We study the dispersion of spinon excitations and the momentum density distribution of one-dimensional Hubbard models in Secs. V and VI, respectively. We discuss the prospects for momentum-space DMRG in the final section.

II. MODEL

The Hubbard model[7] is defined in a general form by the Hamiltonian

$$H=\sum_{i,j,\sigma} t_{ij}c_{i\sigma}^{\dagger}c_{j\sigma}+U\sum_{i} n_{i\uparrow}n_{i\downarrow}, \tag{1}$$

where $c_{i\sigma}^{\dagger}$ ($c_{i\sigma}$) creates (annihilates) an electron with spin σ in the Wannier state on lattice site i with position $\boldsymbol{r}_i$, $n_{i\sigma}=c_{i\sigma}^{\dagger}c_{i\sigma}$ denotes the particle number operator on site i, $t_{ij}=t(\boldsymbol{r}_i-\boldsymbol{r}_j)$ is the transfer integral between site i and j, and U is the energy cost due to the Coulomb repulsion of two electrons on the same site. In this paper, all energies are measured in units of $t=1$.

Using the relation (Fourier transformation) between Wannier states at site i and Bloch states with momentum $\boldsymbol{k}$,

$$c_{\boldsymbol{k}\sigma}^{\dagger}=\frac{1}{\sqrt{N}}\sum_{j} e^{\mathrm{i}\boldsymbol{k}\cdot\boldsymbol{r}_j}c_{j\sigma}^{\dagger}, \tag{2}$$

where N is the number of lattice sites, the Hubbard Hamiltonian with translationally invariant transfer integrals is written in momentum space as

$$H=\sum_{\boldsymbol{k},\sigma}\varepsilon(\boldsymbol{k})n_{\boldsymbol{k}\sigma}+\frac{U}{N}\sum_{\boldsymbol{p},\boldsymbol{k},\boldsymbol{q}} c_{\boldsymbol{p}-\boldsymbol{q}\uparrow}^{\dagger}c_{\boldsymbol{k}+\boldsymbol{q}\downarrow}^{\dagger}c_{\boldsymbol{k}\downarrow}c_{\boldsymbol{p}\uparrow}, \tag{3}$$

where $n_{\boldsymbol{k}\sigma}=c_{\boldsymbol{k}\sigma}^{\dagger}c_{\boldsymbol{k}\sigma}$ and

$$\varepsilon(\boldsymbol{k})=\sum_{j} e^{-\mathrm{i}\boldsymbol{k}\cdot\boldsymbol{r}_j}t(\boldsymbol{r}_j) \tag{4}$$

is the energy dispersion of the electrons.

The kinetic energy of Eq. (3) consists only of diagonal terms with dispersion $\varepsilon(\boldsymbol{k})$, so that the momentum-space DMRG method is trivially exact for $U=0$. Moreover, it can

be easily applied to different noninteracting dispersions $\varepsilon(\boldsymbol{k})$ corresponding to different lattice geometries and hopping ranges. In this paper, we apply the momentum-space DMRG to the following three different models (here and in what follows, we take the lattice constant to be unity and N to be even).

(i) The one-dimensional Hubbard chain with nearest-neighbor hopping amplitude $t_{j+1,j}=-te^{i\phi}$. The dispersion relation is given by

$$\varepsilon(k)=-2t\cos(k-\phi) \tag{5}$$

with $k=2\pi n/N$ and $n=-N/2+1,\ldots,N/2$. The bandwidth is $W=4t$. Here a flux $N\phi$, measured in units of the flux quantum $\phi_0=hc/e$ and equivalent to a twisted boundary condition, is threaded through the system.[8,9] It enables us to calculate the ground-state energy as a function of flux ϕ. We will use nonzero values of ϕ later to interpolate momentum-dependent quantities (e.g., the momentum distribution function) to arbitrary values of the momentum on a finite system.

(ii) The one-dimensional Hubbard chain with long-range hopping amplitude

$$t_{lm}=(-it)\frac{(-1)^{l-m}}{d(l-m)} \tag{6}$$

with

$$d(l-m)=\frac{N}{\pi}\sin\left[\frac{\pi(l-m)}{N}\right]. \tag{7}$$

Since $d(l-m)$ is antisymmetric under the permutation of l and m, the hopping matrix element has to be purely imaginary to guarantee that $t_{lm}=t_{ml}^{*}$. In the thermodynamic limit ($N\to\infty$), the hopping decays proportionally to the inverse of the distance $r=|l-m|$ (''$1/r$ Hubbard model''). The dispersion relation is *linear* and is given by

$$\varepsilon(k)=tk \tag{8}$$

with $k=(2n-1)\pi/N$ and $n=-N/2+1,\ldots,N/2$, where antiperiodic boundary conditions are chosen. The bandwidth is $W=2\pi t$.

(iii) The two-dimensional Hubbard square lattice with nearest-neighbor hopping amplitude $-t$. The dispersion relation is given by

$$\varepsilon(\boldsymbol{k})=-2t(\cos k_x+\cos k_y) \tag{9}$$

with $\boldsymbol{k}=(2\pi n_x/L,2\pi n_y/L)$, where $n_x,n_y=-L/2+1,\ldots,L/2$ and $N=L^2$. The bandwidth is $W=8t$.

The one-dimensional Hubbard model (i) is exactly solvable via the Bethe ansatz[10] and can easily be studied using the real-space DMRG.[11] Comparison with the exact solutions and the real-space method will provide an opportunity to test the performance of the momentum-space DMRG. The $1/r$ Hubbard model (ii) is also exactly solvable,[12] but it is difficult to investigate with the real-space DMRG because the hopping is long range and imaginary. For this model, the advantage of the momentum-space approach is clear: one need only change the real, diagonal dispersion $\varepsilon(k)$. We will, therefore, use this model to investigate how a substantial change in the range of hopping affects the momentum-space algorithm. The Hubbard model on a two-dimensional square lattice (iii) will be used to investigate and compare the effects of dimensionality on the momentum-space method and on the real-space method.

III. DMRG IN MOMENTUM SPACE

In principle, the usual DMRG (Refs. 2 and 3) can be applied directly to the momentum-space representation of the Hubbard model (3). In the momentum-space approach each Bloch function with momentum k and spin σ corresponds to a lattice site. To perform the calculations presented in this paper, we have adapted a program originally written by White.[5] This program predates (and thus does not use) some recent developments that can greatly improve the performance of the DMRG such as the wave-function transformation,[13,3] the use of composite operators,[6] and the use of non-Abelian symmetries.[14] Nevertheless, this program is highly optimized and allows us to carry out DMRG calculations keeping up to $m=4000$ density-matrix eigenstates on a workstation with 1 GB of memory. Below and in the next section we discuss features of the momentum-space DMRG which differ from the usual real-space DMRG.

The summation in the second term of Eq. (3) runs over N^3 products of operators. A straightforward implementation of the DMRG algorithm requires calculating and keeping track of $O(N^3)$ matrices representing the different products of operators. This represents a significant increase compared to the real-space approach that requires only a constant number of operators for the one-dimensional and $O(L=\sqrt{N})$ matrices for the two-dimensional Hubbard model (1), respectively. Xiang[6] has shown that is it possible to define so-called composite operators and thus reduce the number of operators that need to be kept to $6N$. In White's program, internal sums over blocks are carried out to reduce the number of operators to $O(N^2)$ rather than $O(N)$, and an efficient representation of operators with small sparse matrices is used.

We explicitly use the conservation of the particle number $N_e=\Sigma_{\boldsymbol{k},\sigma}n_{\boldsymbol{k}\sigma}$, of the z component of the total spin $S_z=(1/2)\Sigma_{\boldsymbol{k},\sigma}\sigma n_{\boldsymbol{k}\sigma}$, and of the total momentum

$$\boldsymbol{K}=\sum_{\boldsymbol{k},\sigma}\boldsymbol{k}n_{\boldsymbol{k}\sigma}\ \mathrm{mod}2\pi. \tag{10}$$

Momentum symmetry reduces the size of the effective Hilbert space by about a factor N and allows us to decompose the matrix representations of operators into several smaller matrices. Therefore, the dimension of the effective Hilbert space for a given number m of density matrix eigenstates is smaller in the momentum-space approach than in the real-space approach. This should be kept in mind when comparing results obtained with both approaches: In general, m can be made larger for a given amount of computational effort in momentum space.

In a one-dimensional system in real space, there is a natural ordering of the lattice sites. In two dimensions, there is some choice in the ordering,[11,15] but reasonable choices yield similar results.[16] In momentum space it is not *a priori* clear

how one should arrange the sites in the lattice.[6] Thus, we have tested several possibilities including random ordering. We have found that the order of sites should be carefully chosen in the momentum-space approach—the rate of convergence and the accuracy strongly depends on the site order. Fundamentally, it seems that Bloch states that are strongly scattered by the Hubbard term in Eq. (3) should be arranged to be as close together as possible. For the one-dimensional and two-dimensional Hubbard models with nearest-neighbor hopping, we use an energetic ordering in which the sites are arranged according to $|\varepsilon(\boldsymbol{k})-\varepsilon_F|$, where ε_F denotes the Fermi energy in the noninteracting case ($U=0$). For the $1/r$ Hubbard model, the Fermi energy has no particular relevance for low-energy scattering processes and we have found that ordering the sites according to $\varepsilon(k)$ works best.

We use the finite-system DMRG algorithm and perform several sweeps through the lattice until the ground-state energy converges as in the real-space approach. Wilson's numerical RG method is used instead of the infinite system algorithm to build up the lattice during the initial iteration. For the next iterations we apply the usual blocking scheme with a superblock made of two sites and two blocks with at most m states each. In Ref. 6 the superblock was built using two blocks and a single site. According to Xiang, this single-site approach is faster than the usual blocking scheme. As discussed in Ref. 2, however, the single-site blocking scheme is not a robust method unless several states are targeted. As we always target a single state in our calculations [the ground state for some quantum numbers $(N_e,S_z,\boldsymbol{K})$], we use the two-site blocking scheme.

We have observed that the DMRG has difficulty finding the ground state when the interaction U is not weak or for some particular choices of the quantum number $(N_e,S_z,\boldsymbol{K})$. The DMRG sometimes seems to converge first to a state other than the ground state and only converges to the true ground state after many sweeps or after the number m of density-matrix eigenstates is increased. This behavior is marked by a rapid drop in the energy after a relatively large number of sweeps or at a high value of m. A similar problem has been reported with the real-space DMRG applied to two-dimensional fermion systems.[17,18] Therefore, one should not rely on DMRG results obtained for a fixed number m of density-matrix eigenstates kept or a fixed number of sweeps, but one should investigate the behavior of the DMRG as a function of m and of the number of sweeps.

IV. CONVERGENCE AND ACCURACY OF MOMENTUM-SPACE DMRG

In this section we discuss the convergence and accuracy of the momentum-space DMRG method applied to the Hubbard model (3). We have also applied the real-space DMRG method to the real-space representation (1) of the Hubbard Hamiltonian with periodic boundary conditions. This allows us to make comparisons of both DMRG methods in order to illustrate both their differences and their common features. Our real-space DMRG program uses more advanced techniques and is better optimized than our momentum-space DMRG program. Therefore, we have chosen to present no comparison of computer CPU time and memory usage in this paper as they would be meaningless.

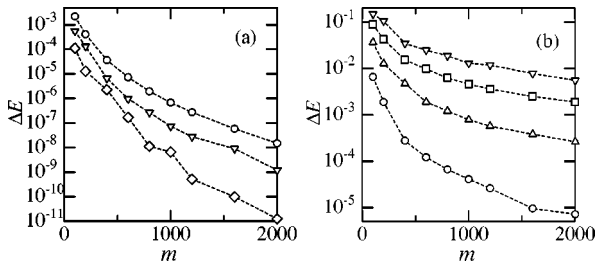

FIG. 1. DMRG error in the ground-state energy of the half-filled one-dimensional Hubbard model with 16 sites and periodic boundary conditions as a function of the number m of density-matrix eigenstates kept in (a) the real-space approach for $U/t=1$ (circles), 4 (reverse triangles), 8 (diamonds), and (b) the momentum-space approach for $U/t=1$ (circles), 2 (triangles), 3 (squares), 4 (reverse triangles).

As a measure of the DMRG precision we use the error in the ground-state energy per site

$$\Delta E(m)=\frac{E_{\mathrm{DMRG}}(m)-E_{\mathrm{exact}}}{Nt}, \tag{11}$$

where E_{exact} is the exact ground-state energy [for particular quantum numbers $(N_e,S_z,\boldsymbol{K})$] and $E_{\mathrm{DMRG}}(m)$ is the corresponding DMRG energy obtained with m density-matrix eigenstates kept. The exact results E_{exact} are calculated using the Bethe ansatz for the one-dimensional Hubbard model[10] and are numerically computed using exact diagonalization techniques for the two-dimensional Hubbard model.[19] For the $1/r$ Hubbard model they are derived from a conjectured effective Hamiltonian.[12] Consistency of the DMRG energies with the spectrum obtained from the effective Hamiltonian in turn confirms the conjecture.

Figures 1(a) and 1(b) show the ground-state energy error ΔE of the one-dimensional Hubbard model as a function of the number of density-matrix eigenstates m for several values of U/t. These results have been obtained on 16-site lattices with periodic boundary conditions at half filling using the real-space [see Fig. 1(a)] and the momentum-space [Fig. 1(b)] approaches. The error ΔE of the momentum-space DMRG method clearly increases with U/t. The error in the real-space DMRG increases with *decreasing* U/t for this half-filled system. In the momentum-space DMRG, the procedure becomes exact when the off-diagonal interaction terms vanish (i.e., at $U=0$) and should be more accurate when they are small—it is a weak-coupling method. In contrast, the real-space representation becomes exact (i.e., local) when $t\to 0$. It is important to note that this is not equivalent to the large U/t limit, in which the real-space DMRG does *not* become exact. The increase in accuracy with U/t shown here is specific to the half-filled insulator, in which the charge degrees of freedom become increasingly localized with increasing U/t. In fact, in the one-dimensional system away from half band filling, there is *very little* dependence of the convergence on U/t (for open boundary conditions).[20] In both approaches, $\Delta E(m)$ does not decrease exponentially as

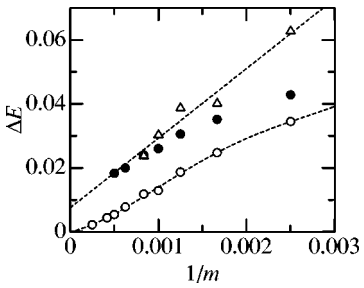

FIG. 2. DMRG error in the ground-state energy as a function of the number m of density-matrix eigenstates kept for the 16-site one-dimensional Hubbard model at half filling with $U/t=4$, including our results for momentum $K=\pi$ (open circles) and $K=0$ (filled circles) and Xiang's results (Ref. 6) for unspecified momentum (triangles). The dashed lines are guides to the eye.

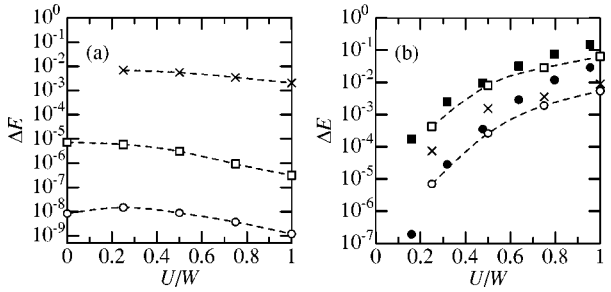

FIG. 3. DMRG errors in the ground-state energy at half filling as a function of the interaction strength U/W calculated with $m=2000$ density-matrix eigenstates. The dashed lines are guides to the eye. (a) Real-space DMRG results for the Hubbard model on a one-dimensional lattice with 16 sites (circles) and 32 sites (squares), and on a two-dimensional 4×4 lattice (crosses). (b) Momentum-space DMRG results for the one-dimensional Hubbard model with 16 sites (open circles) and 32 sites (open squares), the $1/r$ Hubbard model with 16 sites (filled circles) and 32 sites (filled squares), and the two-dimensional Hubbard model on a 4×4 lattice (crosses).

m increases, contrary to the behavior often reported for real-space DMRG calculations on one-dimensional systems with open boundary conditions. In Figs. 1(a) and 1(b) we also see that the errors of the real-space approach are smaller and decrease more rapidly with m than the errors of the momentum-space approach.

In Xiang's work,[6] the systematic convergence of the momentum-space method seems to break down when the interaction strength U approaches the band width W. In particular, for the half-filled Hubbard model on a one-dimensional 16-site lattice with $U/t=4$, the ground-state energy obtained from the DMRG, shown in Fig. 2, does not seem to converge smoothly toward the exact ground-state energy as the number m of retained density-matrix eigenstates is increased—the results are oscillatory and hard to extrapolate. While the origin of this irregular convergence in Xiang's data is unclear, one factor that is essential to consider is that the momentum of the ground state for a half-filled ring with 16 sites and periodic boundary conditions is $K=\pi$ because it is an open-shell configuration. Our results for $K=\pi$ do converge smoothly to the exact solution as a function of $1/m$, as seen in Fig. 2. The lowest-energy state with $K=0$, also shown in the figure, lies closer to Xiang's results for the larger values of m, but converges smoothly to an energy that is clearly higher than the ground state. The deviation of Xiang's result could either be due to his ground state having a different momentum or due to convergence of the the DMRG to a state other than the ground state, as discussed in the previous section.

For weaker interaction, $U/t=1$, Xiang's results converge to the ground-state energy for $K=\pi$, but lie significantly above our own results for the same number of density-matrix eigenstates kept. For instance, the DMRG error in the ground-state energy $\Delta E(m)$ for $m=1200$ is one order of magnitude smaller in our calculations than the value reported by Xiang. This also suggests an incomplete convergence of DMRG in Xiang's calculations even for weak coupling. However, it should also be kept in mind that in his work Xiang used a different superblock structure with a single site between two blocks. As a consequence, the dimension of the effective Hilbert space for a given number of states m is smaller in Xiang's calculations than in our calculations. This difference could be responsible for the better accuracy of our results in the weak-coupling limit $(U/t=1)$ but cannot explain the discrepancy observed for intermediate coupling $(U/t=4)$.

In our calculations, we have often observed that the DMRG energy initially seems to converge towards a value larger than the exact ground-state energy. Upon further increasing the number of states m or the number of sweeps, it then converges to the exact result. In all the cases we present here, the momentum-space DMRG yields energies that *do* ultimately converge to the exact result, even for very large interaction strength U, although the rate of this convergence and the accuracy deteriorate rapidly as U increases.

A. Dependence on model parameters

In this section, we discuss the dependence of the accuracy of the energy of momentum-space DMRG on the model parameters: the single-electron dispersion $\varepsilon(\boldsymbol{k})$, the interaction strength U/W, the lattice dimensionality, and the band filling. Figures 3(a) and 3(b) show the ground-state energy error ΔE as a function of the interaction strength U/W for a fixed number $m=2000$ of density-matrix eigenstates. We again see that errors decrease in the real-space approach [Fig. 3(a)] but increase in the momentum-space approach [Fig. 3(b)] for increasing U/W. In both cases errors increase with the system size and are larger in two dimensions than in one dimension for the same number of lattice sites. However, the dependence on system size and dimensionality of the momentum-space approach is clearly weaker than in the real-space approach. The lower precision of the DMRG in higher dimension is easily understood as a consequence of increasing off-diagonal coupling in the real-space approach. A possible explanation for the slight decrease in accuracy with dimension in the momentum-space representation is that although the single-electron dispersion $\varepsilon(\boldsymbol{k})$ remains diagonal for any dimension, a larger proportion of single-electron states are close to the Fermi surface and are thus strongly

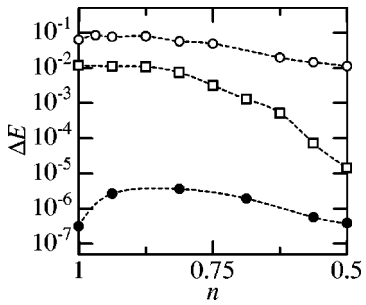

FIG. 4. DMRG error in the ground-state energy as function of band filling n in the one-dimensional Hubbard model for $U/t=4$ on lattices with 16 sites (squares) and 32 sites (circles). Open symbols represent the momentum-space DMRG results and filled symbols for the real-space DMRG results. Real-space DMRG errors for 16 sites are smaller than 10^{-7} and not shown. The number of density-matrix states is $m=1200$ and $m=2000$ for the 16-site and 32-site system, respectively.

scattered. In Figs. 3(a) and 3(b) one also sees that the precision of the real-space approach is generally better than that of the momentum-space approach in the one-dimensional Hubbard model. The latter becomes more accurate than the former for $U/t \lesssim 1$ only. In two dimensions, however, the real-space approach performs very poorly for periodic boundary conditions. The momentum-space approach yields better results for $U \lesssim W=8t$. We finally note that DMRG errors seem to be affected only a small amount by the form of the dispersion $\varepsilon(\boldsymbol{k})$ in the momentum-space approach. In the real-space approach, however, changing the single-electron dispersion by introducing longer-range hopping lowers the DMRG performance very rapidly. In summary, we find that the momentum-space approach is superior to the real-space approach for applications to translationally invariant systems with weak-to-intermediate Coulomb interactions in two dimensions or on one-dimensional lattices with long-range hopping.

Let us now consider the effects of the band filling. In Fig. 4 we show the error ΔE in the ground-state energy as a function of band filling $n=N_e/N$ for the one-dimensional Hubbard model at $U=4t$. In the momentum-space approach, the accuracy is worst at or near half filling and improves as the density decreases from $n=1$. One cause of this effect is that the size of the Hilbert space is maximal at half filling and decreases rapidly at large doping. This effect is magnified in the 16-site system relative to the 32-site system, as seen in Fig. 4, because a substantial proportion of the Hilbert space is retained in the diagonalization step at large doping. Another possible cause is the reduction in the effective strength of the electron-electron scattering as the system is doped away from half filling. The effective interaction strength depends on the ratio of U and the density of states at the Fermi energy, which becomes smaller with doping, in weak coupling. As the effective interaction becomes smaller, the electrons become more localized in momentum space, which should be favorable for the convergence of the momentum-space DMRG. In the real-space approach, Fig. 4 shows that the error in the ground-state energy first increases as the system is doped slightly away from half filling, then decreases upon further doping. As discussed previously, the charge degrees of freedom are localized in the half-filled insulator, leading to improved convergence for the real-space algorithm. For any finite doping, the system immediately becomes metallic, i.e., some charge degrees of freedom become delocalized, leading to a reduction in accuracy. As the system is doped further from half filling, the reduction in the size of the Hilbert space leads to an improvement in accuracy, as in the momentum-space approach.

Extrapolation to $m \to \infty$

DMRG calculations have a truncation error that is reduced by increasing the number m of density-matrix eigenstates kept.[2,3] It is important to analyze the scaling of DMRG results as a function of m to estimate DMRG errors quantitatively. In real-space DMRG calculations, one generally observes that energy errors $\Delta E(m)$ are proportional to the discarded weight P_m,[18,21] provided that the DMRG has converged to the right target state. Here the discarded weight P_m is defined as the total weight (sum of the density-matrix eigenvalues) of the discarded density-matrix eigenstates, averaged over a sweep through all lattice sites in the finite-system DMRG algorithm. Thus, it is possible to extrapolate DMRG eigenenergies to the limit $P_m \to 0$. This procedure produces extrapolated energies that are closer to the exact eigenenergies than the DMRG energies calculated for a given value of m. Moreover, the extrapolation yields reliable quantitative error margins for the eigenenergies.

In momentum space, however, we have found that the linear relationship between the energy errors $\Delta E(m)$ and P_m often does not hold, even for small P_m. In fact, we find that the dependence of P_m on m can even be nonmonotonic. An extrapolation to vanishing discarded weight $P_m \to 0$ is therefore, generally not possible. That such a nonmonotonic behavior is found at all is surprising at first glance because the discarded weight P_m of the *exact* density matrix for the system decreases monotonically with increasing m per definition. An exact density matrix for the ground state of the Hubbard model can be calculated numerically in small systems using exact diagonalization. Using the results of such a calculation on a $N=12$ lattice, we have found that the density-matrix eigenvalues $w_i, i=1,2,\ldots$ appear to decrease exponentially as a function of i in the asymptotic regime $i \gg 1$. As a consequence, the exact discarded weight $P_m=\Sigma_{i=1}^{m} w_i$ and the corresponding energy error $\Delta E(m)$ must also decrease exponentially with increasing m. This is observed for density matrices calculated in the momentum-space approach as well as those obtained in the real-space approach (both for open and periodic boundary conditions). Such an exponential falloff of the density-matrix eigenvalues has been found for exactly solvable models.[16] In an actual DMRG calculation, however, the density matrix is calculated self-consistently. Thus different density matrices can be obtained for different m, and P_m can, in principle, be an arbitrary function of m, except for the condition $\lim_{m\to\infty} P_m=0$. We expect such effects to be largest where P_m is large and the self-consistently determined density matrix is a poor approximation to the exact one.

In the momentum-space approach, the error in the DMRG energy $\Delta E(m)$ does not decrease exponentially with increas-

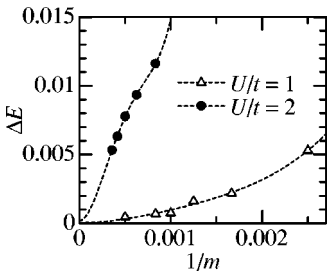

FIG. 5. DMRG error in the ground-state energy as a function of $1/m$ for the one-dimensional Hubbard model on a 32-site lattice. The lines are least-square fits to a fourth-order polynomial, $n=4$ in Eq. (12).

ing m, but rather shows a power-law behavior in $1/m$ in the limit $m \gg 1$. We, therefore, extrapolate the momentum-space DMRG results to vanishing truncation error by performing a least-squares fit of the DMRG energies $E_{\mathrm{DMRG}}(m)$ for several m to a nth order polynomial in $1/m$,

$$E_{\mathrm{fit}}\left(\frac{1}{m}\right) = E_\infty + \frac{a_1}{m} + \frac{a_2}{m^2} + \cdots + \frac{a_n}{m^n}. \tag{12}$$

An extrapolated energy for vanishing truncation errors ($m \to \infty$) is given directly by the fit parameter E_∞. The energy $E_{\mathrm{DMRG}}(m)$ must be a monotonically decreasing function of m since the DMRG is a variational method and increasing m means increasing the variational subspace dimension. Therefore, $E_{\mathrm{DMRG}}(1/m)$ must satisfy the constraint $dE_{\mathrm{DMRG}}(x)/dx > 0$ for x in the range $0 < x \leqslant 1/m' \leqslant 1$, where m' is smaller than or equal to the smallest value of m used in the fit. An obvious consequence of this constraint is that the first-order term in the polynomial $E_{\mathrm{fit}}(1/m)$ must satisfy $a_1 \geqslant 0$. We have found that the best fit under this constraint systematically gives $a_1 = 0$.

Figure 5 shows the DMRG errors ΔE in the ground-state energies of the one-dimensional 32-site Hubbard model for $U/t=1$ and 2 and the results of least-square fits to a fourth-order polynomial, $n=4$ in Eq. (12). The DMRG errors $\Delta E(m)$ for the largest value of m used are 4.5×10^{-4} ($m=2000$) and 5.3×10^{-3} ($m=2800$) for $U/t=1$ and $U/t=2$, respectively. The accuracy is greatly improved by the polynomial fit and the $m\to\infty$ extrapolation. The errors in the corresponding extrapolated ground-state energies per site are 2.9×10^{-5} for $U/t=1$ and 4.5×10^{-5} for $U/t=2$.

To illustrate the benefit of extrapolating DMRG energies to vanishing truncation errors we now consider the quasiparticle gap Δ_{qp} of the one-dimensional Hubbard model at half filling. The quasiparticle gap is defined by

$$\Delta_{\mathrm{qp}} = E_0(N+1;N) + E_0(N-1;N) - 2E_0(N;N), \tag{13}$$

where $E_0(N_e;N)$ is the ground-state energy of a system with N sites and N_e electrons with minimal S_z, i.e., $N_\uparrow = N_\downarrow$ or $N_\uparrow = N_\downarrow + 1$. The charge conjugation symmetry of the Hubbard model implies that $E_0(N+1;N) = E_0(N-1;N) + U$, so only one of these two energies need be computed. Some results for Δ_{qp} are shown in Table I. If one calculates the quasiparticle gap with the DMRG results for $E_0(N_e;N)$ obtained for fixed values of m, the magnitude of errors in Δ_{qp} fluctuates widely. The origin of this behavior has two competing sources. On the one hand, DMRG errors in the eigenenergies $E_0(N_e;N)$ tend to be systematic for similar values of N and N_e and cancel when calculating Eq. (13). Thus, the absolute error in Δ_{qp} can be smaller than the error in $E_0(N_e;N)$ as seen in Table I for the case $U=2t$. On the other hand, the eigenenergies are extensive quantities [i.e., $E_0(N_e;N)$ scales with N for constant density N_e/N], while Δ_{qp} is an intensive quantity (i.e., Δ_{qp} tends to a constant for increasing N and constant density N_e/N). Thus, even small but nonsystematic errors in $E_0(N_e;N)$ immediately result in much larger relative errors in Δ_{qp}. As a consequence, the values of Δ_{qp} (or similar physical quantities) obtained for a given number of density-matrix eigenstates kept might be accurate but there is considerable uncertainty about their accuracy. The extrapolation of the ground-state energies $E_0(N_e;N)$ to vanishing truncation errors allows us to eliminate this uncertainty and even to improve the precision of our results. For instance, in Table I one can see that the errors in Δ_{qp} calculated with extrapolated ground-state energies are up to one order of magnitude smaller than for the largest value of m used ($m=2000$).

TABLE I. Ground-state energies and quasiparticle gap, Eq. (13), for the one-dimensional Hubbard model with $N=32$ sites.

U/t		$m=2000$	Extrapolated	Exact
1	$E_0(N;N)/t$	−33.20078	−33.21423	−33.21515
	$E_0(N+1;N)/t$	−32.64191	−32.65757	−32.65687
	Δ_{qp}/t	0.12186	0.11472	0.11515
2	$E_0(N;N)/t$	−26.80161	−27.01970	−27.01826
	$E_0(N+1;N)/t$	−25.61577	−25.83275	−25.83170
	Δ_{qp}/t	0.37737	0.37390	0.37311

V. DISPERSION OF SPINON EXCITATIONS

An advantage of the momentum-space method is that momentum-dependent quantities can be easily calculated. In this section, we investigate the dispersion of the spinon excitation $E_s(k)$ at half band filling for both the one-dimensional Hubbard model with nearest-neighbor hopping and the $1/r$ Hubbard model; the spinon spectrum is known exactly in both cases.

The lowest spin-triplet excitation with momentum k in a system of size N with a singlet ground state is given by

$$\varepsilon_t(k;N) = E_0(N_e/2+1, N_e/2-1, k+k_0;N) - E_0(N_e/2, N_e/2, k_0;N), \tag{14}$$

where $E_0(N_\uparrow, N_\downarrow, k;N)$ denotes the energy of the lowest state with $N_\uparrow$ ($N_\downarrow$) up-spin (down-spin) electrons and total momentum k, and k_0 is the momentum of the singlet ground state. In one-dimensional spin-1/2 systems, a spin-triplet excitation is composed of two or more spin-1/2 spinons that are gapless in the thermodynamic limit. Therefore, the lowest-energy spin-one excitation allows us to map out the spinon dispersion as a function of momentum,

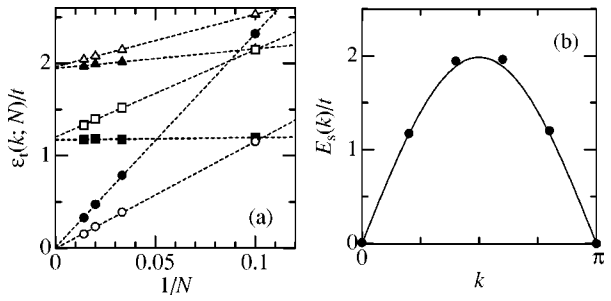

FIG. 6. Spin excitations in the one-dimensional Hubbard model at half filling for $U/t=0.4$. (a) Energy $\varepsilon_t(k;N)$ of the lowest triplet excitation calculated with DMRG as a function of the inverse system size $1/N$ for momenta $k=0$ (filled circles), 0.2π (filled squares), 0.4π (filled triangles), 0.6π (open triangles), 0.8π (open squares), and π (open circles). Dashed lines are linear fits in $1/N$. (b) Spinon dispersion $E_s(k)$ in the thermodynamic limit $N\to\infty$. The circles show the results obtained by extrapolation of the DMRG data in (a) [see Eq. (15)]. The solid line is the exact result obtained in Ref. 22.

$$E_s(k)=\varepsilon_t(k;N\to\infty), \quad 0\leqslant k\leqslant\pi. \tag{15}$$

In Fig. 6(a), we show the lowest triplet excitation $\varepsilon_t(k;N)$ of the half-filled Hubbard model with nearest-neighbor hopping at $U/t=0.4$ for several momenta k and system sizes N up to 70 sites. The excitation energies scale approximately linearly with $1/N$ for all momenta but the slope varies considerably for the different k. This finite-size scaling is readily understood from the exact result at $U=0$ for a closed-shell system,

$$\varepsilon_t(k;N)=2t\sin(k)+8t\sin\left(\frac{k}{2}\right)\sin\left(\frac{\pi}{2N}\right)\sin\left(\frac{k}{2}-\frac{\pi}{2N}\right), \tag{16}$$

where $k=2\pi n/N$ and $n=1,\ldots,N/2$. We, therefore, extrapolate the energies $\varepsilon_t(k;N)$ to the thermodynamic limit using a linear fit in $1/N$ to obtain the spinon dispersion $E_s(k)$ though Eq. (15). The results for $E_s(k)$ are shown in Fig. 6(b) and compared with the exact spinon dispersion[22] for $U/t=0.4$. One sees that our numerical results for $E_s(k)$ agree very well with the analytical curve. In particular, $\varepsilon_t(k=0,\pi;N\to\infty)=0$ within the accuracy of the extrapolation. Note that because of the weak interaction $U=0.4t$ considered in this example, DMRG is very accurate and extrapolation of eigenenergies as a function of the number m of density-matrix states is not necessary. Thus, we have used fixed numbers of states $m=400, 800, 1200, 2000$ for $N=10, 30, 50, 70$, respectively. Actually, errors due to the infinite-system extrapolation are at least an order of magnitude larger than the DMRG error in the ground-state energy (per site), which is 2.7×10^{-4} in the worst case, $N=70$.

In the $1/r$ Hubbard model, the spinon spectrum at half band filling is given by[12]

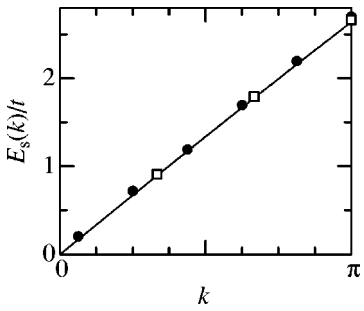

FIG. 7. Spinon spectrum $E_s(k)$ of the $1/r$ Hubbard model for $U/t=1$. DMRG results for finite systems with $N=24$ sites (squares) and $N=32$ sites (circles). The solid curve is the exact result for an infinite system [Eq. (17)].

$$E_s(k)=\frac{1}{4}\left(\sqrt{W^2+U^2-\frac{4WU}{\pi}\left(k-\frac{\pi}{2}\right)}+\frac{2W}{\pi}\left(k-\frac{\pi}{2}\right)\pi-U\right), \quad 0\leqslant k\leqslant\pi \tag{17}$$

in the thermodynamic limit. In order to form the lowest spin-triplet excitations, two spinon excitations are necessary. If they have momenta $k_1=k$ and $k_2=0$, the spin-triplet excitation will have total momentum k and excitation energy $\varepsilon_t(k)=E_s(k)$ with respect to the ground state, as $E_s(k_2=0)=0$. In Fig. 7, this analytical result for an infinite system is compared to our momentum-space DMRG results in finite systems of size $N=24$ and $N=32$ for $U/t=1$. We observe an almost perfect agreement, implying the absence of significant finite-size effects. This is a consequence of the linear dispersion and weak coupling considered here. It can be inferred from the results of Ref. 12 that the dispersion of spin-triplet excitations has no explicit dependence on the system size to first order in U/W

$$\varepsilon_t(k;N)=tk\left(1-\frac{U}{W}\right). \tag{18}$$

Therefore, the finite-size corrections are of the order $(1/N)\times(U/W)^2\ll1$ and are negligible in the results for $U/t=1$ and $N\geqslant24$ presented in Fig. 7. As in the nearest-neighbor hopping case, DMRG errors in the energy are negligibly small compared to the spinon bandwidth because of the weak interaction used here. Thus in Fig. 7 we show DMRG results for a fixed number m of density-matrix states ($m=800$ for $N=24$ and $m=1600$ for $N=32$) instead of results extrapolated to the $m\to\infty$ limit. These results, along with the results for the one-dimensional Hubbard model discussed previously, show that the low-lying spin-excitation spectrum can be accurately calculated using the momentum-space DMRG, at least in the weak-coupling limit.

VI. MOMENTUM DISTRIBUTION

Another quantity that is easily accessible to the momentum-space DMRG is the single-particle momentum distribution

$$n(k)=\frac{1}{2}\sum_{\sigma}\langle n_{k\sigma}\rangle. \tag{19}$$

We have calculated $n(k)$ in the ground state of the one-dimensional Hubbard model with nearest-neighbor hopping and of the $1/r$ Hubbard model at half band filling using DMRG. Since DMRG truncation errors are typically larger for quantities such as $n(k)$ than for eigenenergies, it is crucial to examine the effect of varying m. The relative size of the finite-size effects is also important because one is interested in the behavior of $n(k)$ in the thermodynamic limit. In the following, we compare our DMRG results to analytic results for $n(k)$ on infinite lattices in the limit of both large and small interaction strength.

A. Nearest-neighbor hopping

In the ground state of the one-dimensional Hubbard model with nearest-neighbor hopping, the distribution $n(k)$ is symmetric, $n(-k)=n(k)$. Therefore, we show results for $0\leqslant k\leqslant\pi$ only.

We compare our DMRG results with an approximate expression for $n(k)$ proposed recently by Koch and Goedecker.[23] They make the ansatz that the real-space one-particle density matrix $\langle c^{\dagger}_{i\sigma}c_{j\sigma}\rangle$ of the interacting system can be written as a product of the density matrix for the noninteracting system and an exponential decay factor that is a function of the particle-hole distance. The corresponding momentum distribution is

$$n_{\mathrm{KG}}(k)=\frac{1}{2}+\frac{1}{\pi}\arctan\left(\frac{\cos(k)}{\sinh(\gamma)}\right). \tag{20}$$

Here $1/\gamma$ denotes the decay length and is given by

$$\frac{e^{-\gamma}}{\pi}=\langle c^{\dagger}_{i+1\sigma}c_{i\sigma}\rangle=\int_0^{\infty}dx\,\frac{J_0^2(x)-J_1^2(x)}{1+\exp(Ux/2t)}, \tag{21}$$

where $J_0(x)$ and $J_1(x)$ are Bessel functions of the first kind. In Ref. 23 it is found that exact diagonalization calculations on systems of up to 16 sites agree well with this form for $U/t\gtrsim 6$. For smaller U/t, deviations are seen for wave vectors $k\approx k_F$.

Expansion of Eq. (21) in the strong-coupling limit yields

$$\gamma=-\ln\left(\frac{2t\pi\ln 2}{U}\right) \tag{22}$$

and one recovers the perturbative result[24]

$$n(k)=\frac{1}{2}-\frac{2\ln(2)\varepsilon(k)}{U};\quad U\gg t. \tag{23}$$

In Fig. 8, we compare Eq. (20) for $k>0$ with the momentum-space DMRG results for $U/t=10$ and $U/t=20$ on small finite lattices. We use periodic boundary conditions ($\phi=0$) for systems with $N=4n+2$ sites and antiperiodic boundary conditions ($\phi=\pi/N$) for system with $N=4n$ sites (where n is an integer) to ensure closed-shell configurations. The momentum-space DMRG calculations agree reasonably well with the analytical result, but we note that the agreement becomes less good with increasing system size for $U/t=20$. An analysis of the behavior for different m shows that our DMRG results underestimate $n(k)$ for $|k|<k_F=\pi/2$ and overestimate $n(k)$ for $|k|>k_F$. Therefore the deviations seen in Fig. 8 are a consequence of DMRG errors which become larger for the larger system sizes and we would expect all results to lie on the analytic curve as in Ref. 23 in the $m\to\infty$ limit.

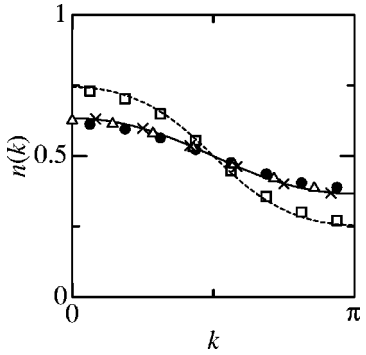

FIG. 8. Ground-state momentum distribution function $n(k)$ of the one-dimensional half-filled Hubbard model at $U/t=20$ for system sizes $N=12$ (crosses), $N=14$ (triangles) and $N=16$ (circles) keeping $m=2000$ states, and at $U/t=10$ for $N=16$ sites (squares) keeping $m=1200$ states. The lines correspond to the ansatz (20).

In the limit of weak coupling, γ is given by[25]

$$\gamma\approx 7\zeta(3)\left(\frac{U}{8\pi t}\right)^2, \tag{24}$$

where $\zeta(z)$ is the Riemann zeta function [$\zeta(3)\approx 1.2$]. In Fig. 9 we compare Eq. (20) with our DMRG results for $U/t=1$ and $U/t=2$ on a 70-site lattice. We superimpose results with different phases $0\leqslant\phi<2\pi/N$ to obtain better resolution in the vicinity of the Fermi momentum $k_F=\pi/2$. Note that we

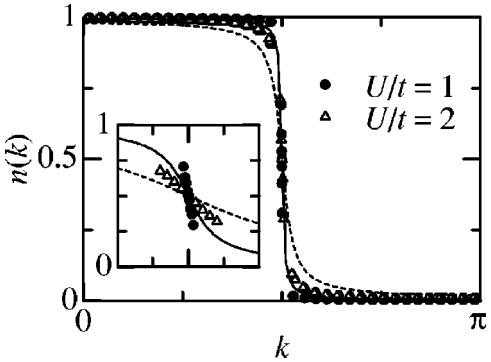

FIG. 9. Single-particle momentum distribution of the one-dimensional half-filled Hubbard model on a 70-site lattice for different phases ϕ. The circles are for $U/t=1$ (with $m=800$ states kept) and the triangles for $U/t=2$ (with $m=1200$ states kept). The lines correspond to Eq. (20) for $U/t=1$ (solid) and $U/t=2$ (dashed). The inset shows a blowup of the region [$\pi/2-0.0143\pi,\pi/2+0.0143\pi$] around the Fermi momentum.

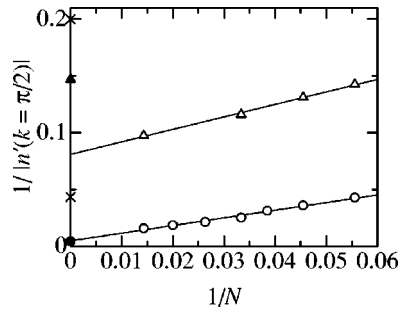

FIG. 10. Inverse of the slope at the Fermi wave vector $1/|n'(k=\pi/2)|$ as a function of inverse system size $1/N$ for $U/t=1$ (open circles) and $U/t=2$ (open triangles). The lines are linear fits to the DMRG data. The filled symbols are the corresponding field-theoretic results and the crosses are calculated from the Koch-Goedecker ansatz (20).

can do this only in the insulating phase where the dependence of the ground state on the phase ϕ is negligible for small ϕ because the Drude weight[8,9] (which is proportional to $\partial^2 E_0/\partial\phi^2|_{\phi=0}$) vanishes. Unlike the limit of strong coupling, the agreement between our DMRG data and Eq. (20) is not good near k_F, as seen in the inset of Fig. 9. The first derivative of $n(k)$ at $k=k_F$ is $n'(k_F)\approx -64$ at $U/t=1$ and $n'(k_F)\approx -10.3$ at $U/t=2$, whereas Eq. (21) yields $n'_{\mathrm{KG}}(k_F)=-23$ at $U/t=1$ and $n'_{\mathrm{KG}}(k_F)=-5.0$ at $U/t=2$. Although the ansatz (20) correctly describes the overall shape of $n(k)$ deep in the insulating regime ($U/t\gtrsim 6$), we find that it does not quantitatively recover the $U/t\to 0$ and $|k-k_F|\to 0$ scaling limit.

The behavior of the slope in the scaling limit can be understood by examining the Green function for the sine-Gordon model.[26] The Fourier transform of the equal-time Green function becomes[27]

$$n_{\mathrm{ft}}(k\gtrless 0)=\frac{1}{2}-\frac{Z_0}{\pi}\arctan\left(\frac{v_h(k-\pi/2)}{\Delta_{\mathrm{qp}}/2}\right), \tag{25}$$

where $v_h=2t$ is the holon velocity and $Z_0=0.9219$ has been calculated in Ref. 28. The slope at $k=k_F=\pi/2$ is then given by

$$n'_{\mathrm{ft}}(k=k_F)=-\frac{4Z_0}{\pi\Delta_{\mathrm{qp}}}, \tag{26}$$

which has the values $n'_{\mathrm{ft}}(k=k_F)=-233$ at $U/t=1$ and $n'_{\mathrm{ft}}(k=k_F)=-6.8$ at $U/t=2$ when the exact values for Δ_{qp} in the thermodynamic limit[29] are used. In Fig. 10 we show the scaling with inverse system size of the DMRG results for $1/|n'(k=k_F)|$. For $U/t=1$, a $1/N\to 0$ extrapolation (using a linear form) yields $n'(k=k_F)=-207$, which agrees to within the fit errors with the field-theoretic result, corroborating both the field-theoretic and DMRG results in this regime. For $U/t=2$, we obtain $n'(k=k_F)=-12$, whose absolute value is substantially larger (i.e., outside our estimate for the error) than that of the field-theoretic result. We believe that this is because $U/t=2$ is large enough so that the field-theoretic approximation to the momentum distribution of the Hubbard model begins to show significant deviations from the lattice result. This is supported by the fact that the field-theoretic formula (26) correctly reproduces the strong-coupling form (23), but with a prefactor $4Z_0/\pi\approx 1.2$ rather than $4\ln 2\approx 2.8$, indicating that the field-theoretic formula underestimates the slope at larger values of U.

B. $1/r$ hopping

In the ground state of the $1/r$ Hubbard model at half filling, $n(-k)=1-n(k)$. The half-filled model describes a metal for $U<W=2\pi t$ and an insulator for $U>W$.

The momentum distribution in the $1/r$ Hubbard model can be calculated in perturbation theory. For large coupling $U\gg t$, we use Takahashi's approach.[24] To this end, we need the spin-spin correlation function in the Gutzwiller-projected paramagnetic Fermi-sea at half band filling, which is the ground state of the Haldane-Shastry spin chain.[30] The spin-spin correlation function for the Haldane-Shastry model is given by[12,31]

$$\frac{1}{N}\sum_l \langle \boldsymbol{S}_l\cdot\boldsymbol{S}_{l+r}\rangle=(-1)^r\frac{3\mathrm{Si}(\pi r)}{4\pi r}\quad (r\neq 0), \tag{27}$$

where $\mathrm{Si}(x)$ denotes the sine integral. The momentum distribution for large U/t is then

$$\begin{aligned} n(k)&=\frac{1}{2}-\frac{1}{U}\sum_{r=1}^{\infty}(-1)^r\frac{\sin(kr)}{r}\left(\frac{3\mathrm{Si}(\pi r)}{\pi r}-1\right)\\ &=\frac{1}{2}\left[1-\frac{k}{U}\left(1-3\ln\left|\frac{k}{\pi}\right|\right)\right]. \end{aligned} \tag{28}$$

Note that although the momentum distribution is continuous at $k_F=0$, we can expect to observe a large apparent jump in numerical simulations of finite systems even at large U/t because of the sizeable logarithmic term in Eq. (28).

For small couplings, standard perturbation theory in U/t is applicable because the model reduces to a pure g_4 model in the conformal limit.[12] It turns out that the Gutzwiller wave function becomes exact in the small-coupling limit so that the momentum distribution for $U\ll t$ becomes[32]

$$n(k)=\begin{cases} 1-(U^2/W^2)f(k) & \text{for}\quad -\pi<k<0\\ (U^2/W^2)f(k) & \text{for}\quad 0<k<\pi \end{cases} \tag{29}$$

with $f(k)=3/16-[1/4-|k|/(2\pi)^2]$.

Figure 11(a) displays the momentum distribution function for the half-filled $1/r$ Hubbard model for $U/t=20$ on an $N=12$ lattice compared with the strong-coupling result (28), and for $U/t=4$ on an $N=16$ lattice compared with the the weak-coupling result (29). The agreement is very good because the DMRG errors are negligible for such small systems and because the finite-size effects are small, at least on the scale of the figure.

The finite-size effects in weak coupling are more visible in Fig. 11(b). One can see that the perturbation theory, Eq. (29), agrees well with the numerical results at all system sizes for $U/t=1$. However, deviations that become larger with system size can be seen for $U/t=2$. The results for the smaller systems incorrectly suggest that Eq. (29) applies per-

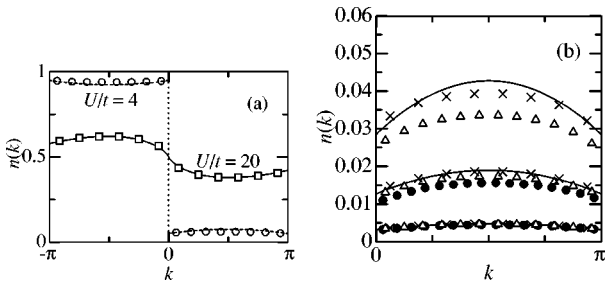

FIG. 11. Momentum distribution function for the $1/r$ Hubbard model at half filling with $m=2000$ states kept. (a) DMRG results on an $N=16$ lattice for $U/t=4$ and an $N=12$ lattice for $U/t=20$. The solid and dashed lines are from the perturbative first-order result in t/U, Eq. (28), and the second-order result in U/t, Eq. (29), respectively. (b) The weak-coupling regime for $U/t=1,2,3$ (from bottom to top). The crosses, open triangles, and filled circles denote $N=16,24,32$. The solid line results from Eq. (29).

fectly and that finite-size effects are absent. This effect is even more marked at $U/t=3$ where the analytic weak-U result agrees almost perfectly with the numerical data for $N=16$, but the data for $N=24$ reveal that the agreement would be worse in the thermodynamic limit. Apparently, the finite-size effects are approximately of the same order and sign as the higher-order corrections in U/t here.

VII. DISCUSSION AND OUTLOOK

In this work, we have examined in detail the application of the density matrix renormalization group to the momentum-space representation of the Hubbard model. We have treated three different dispersion relations corresponding to the one-dimensional chain with nearest-neighbor hopping, the one-dimensional chain with hopping that decays as $1/r$, and the two-dimensional square lattice with isotropic nearest-neighbor hopping. While the one- and two-dimensional nearest-neighbor hopping cases were treated previously by Xiang,[6] here we have extended the scope of his results and have addressed some issues raised by his work. In particular, we have taken advantage of the Bethe ansatz exact solution,[10] which yields the exact ground-state energy to within machine precision for all system sizes, to make more extensive studies of the convergence for the one-dimensional model with the number of density-matrix eigenstates m. We have examined the effect of system size, interaction strength and band filling at up to $m=4000$.

For all parameters and models, we have found systematic variational convergence with m to the true ground state; this does not seem to clearly occur in Xiang's, at least in his $U/t=4$ results for the one-dimensional system. However, the convergence seems to be slower than exponential for the range of m accessible to us. The accuracy decreases regularly with system size when the other parameters are fixed, as one finds for the real-space DMRG. The accuracy also becomes rapidly worse with interaction U, as also found by Xiang. Our more extensive set of interaction strengths indicates that the behavior is quite regular as a function of U; convergence does not break down at a particular U value.

In the one-dimensional Hubbard model with periodic boundary conditions, a comparison with the real-space DMRG applied to the same system with the same m indicates that the accuracy of the real-space method is better for $U/t \gtrsim 1$. The dependence of the accuracy on band filling is weak in momentum space, except on small system sizes for which the proportion of the Hilbert space kept changes drastically with filling.

For the two-dimensional system, we have restricted ourselves to the half-filled 4×4 system, the largest for which exact diagonalization data are available, and have compared with the real-space DMRG. We find that the momentum-space method is more accurate than the real-space method (for the same m) when $U \lesssim 8t=W$.

One crucial issue raised by Xiang is the dependence of the accuracy on dimensionality or, relatedly, the range of the hopping. He speculated that such effects would be smaller for the momentum-space DMRG than for the real-space DMRG, a speculation that we have confirmed here. We emphasize, however, that the choice of values of interaction strength which are compared is important. It is our opinion that a reasonable choice is the interaction divided by the bandwidth, U/W (at identical filling and number of lattice sites). The bandwidth sets the energy scale for many physical phenomena and also is relevant to the strength of the coupling in perturbation theory. (A possibly useful alternative might be the ratio of the interaction strength and the density of states at the Fermi energy, the coupling parameter in weak-coupling perturbation theory.) For given U/W (as opposed to given U/t), the accuracy of the momentum-space DMRG is lower in two dimensions than in one, an effect that becomes smaller as the interaction becomes larger. In one dimension, changing to the longer-range $1/r$ hopping has little effect on the accuracy at weak U/t, although the accuracy does become somewhat worse as U/t is increased. We, therefore, conclude that while the performance of the momentum-space DMRG is less dependent on range of the hopping or dimensionality than the real-space DMRG, there is still some effect.

While the ground-state energy is an important indicator of convergence, it is not a particularly useful quantity in determining the physical behavior of a system. We have, therefore, examined a number of other quantities that are easily accessible to the momentum-space DMRG, which also yield useful physical information. Gaps formed from differences in energies provide important information about the excitation spectrum. We have examined the single-particle gap as well as the momentum-dependent triplet gap for both one-dimensional models at half filling. For the single-particle gap, extrapolation in $1/m$ is crucial in obtaining consistent accuracy because of cancellation of variational errors and because the gap is an intensive quantity obtained by subtracting extensive energies. We have found that a direct extrapolation using a polynomial in $1/m$ is the best method because the error in the ground-state energy is not well correlated with the weight of the discarded density-matrix eigenvalues, unlike in the real-space DMRG. For the spin excitation spectrum, we have treated parameter values for which extrapolation in m is unnecessary and found that the finite-size effects are substantial for the nearest-neighbor-hopping chain. For

the $1/r$-Hubbard model, finite-size effects were quite small. In both cases, the size-extrapolated spectrum agrees well with exact results.

Finally, we have examined the momentum distribution function. For the nearest-neighbor chain, we compare with an analytical ansatz of Koch and Goedecker.[23] At strong coupling, we find very good agreement aside from deviations due inaccuracy of the DMRG results. At weak interaction, the DMRG results agree with field-theoretic results,[26] whereas there is significant deviation from the Koch-Goedecker ansatz. For the $1/r$-Hubbard model, agreement with weak and strong coupling results is good, although finite-size corrections with the same sign as higher order terms in U/t provide better agreement for small system sizes than is justified in the thermodynamic limit.

In summary, the momentum-space DMRG can be a useful tool for the Hubbard model at weak-to-intermediate coupling. While it is competitive with the real-space DMRG only at quite weak coupling for the one-dimensional model (even with periodic boundary conditions), it is competitive up to significantly stronger coupling for longer-range hopping or in two dimensions. It should be noted that the accuracy of the momentum-space DMRG is generally significantly lower than that of the more favorable cases for the real-space DMRG, and can be considered a ''numerically exact'' method only with reservations. It can, however, be a useful variational method where no more exact methods are available if its limitations are well understood. The ease of calculation of momentum-dependent quantities is very useful—such quantities are often not available on large systems even for well-understood models. For these quantities, care must be taken with respect to accuracy and finite-size effects, but we have found them to be well behaved within these limitations.

The momentum-space DMRG code used here is far from maximally optimized. With similar optimizations as used in the real-space program such as the use of wave function transformations to improve the initial guess for the target state in the diagonalization,[13] it should be possible to keep significantly more density-matrix eigenstates for given numerical effort in the momentum-space method than in the real-space method applied to the same system. Use of such a better optimized program might increase the range of applicability of the momentum-space DMRG somewhat. In addition, since the Hubbard model has a local interaction in real-space, the interaction is quite nonlocal in momentum space. The momentum-space DMRG could quite possibly be better suited to models with longer-range interaction in real space, corresponding to more local interactions in momentum space. Such directions would certainly be worth exploring in future work.

ACKNOWLEDGMENTS

This work was supported by the Deutsche Forschungsgemeinschaft under Grant No. GE 746/6-1. We acknowledge helpful discussions with F.H.L Essler, S.R. White, and T. Xiang.

[1] K.G. Wilson, Rev. Mod. Phys. **47**, 773 (1975).
[2] S.R. White, Phys. Rev. Lett. **69**, 2863 (1992); Phys. Rev. B **48**, 10 345 (1993).
[3] *Density-Matrix Renormalization*, edited by I. Peschel, X. Wang, M. Kaulke, and K. Hallberg (Springer, Berlin, 1999).
[4] S.R. White, Phys. Rev. B **45**, 5752 (1992).
[5] S. R. White (private communication).
[6] T. Xiang, Phys. Rev. B **53**, 10 445 (1996); see also T. Xiang and X. Wang, in *Density Matrix Renormalization* (Ref. 3), p. 149.
[7] J. Hubbard, Proc. R. Soc. London, Ser. A **276**, 238 (1963).
[8] W. Kohn, Phys. Rev. **133**, A171 (1964).
[9] B.S. Shastry and B. Sutherland, Phys. Rev. Lett. **65**, 243 (1990).
[10] E.H. Lieb and F.Y. Wu, Phys. Rev. Lett. **20**, 1445 (1968).
[11] R.M. Noack, S.R. White, and D.J. Scalapino, in *Computer Simulations in Condensed Matter Physics VII*, edited by D.P. Landau, K.K. Mon, and H.B. Schüttler (Spinger Verlag, Heidelberg, Berlin, 1994), p. 85.
[12] F. Gebhard and A.E. Ruckenstein, Phys. Rev. Lett. **68**, 244 (1992); F. Gebhard, A. Girndt, and A.E. Ruckenstein, Phys. Rev. B **49**, 10 926 (1994).
[13] S.R. White, Phys. Rev. Lett. **77**, 3633 (1996).
[14] I. McCulloch and M. Gulacsi, Europhys. Lett. **57**, 852 (2002).
[15] T. Xiang, J. Lou, and Zh. Su, Phys. Rev. B **64**, 104414 (2001).
[16] M.-C. Chung and I. Peschel, Phys. Rev. B **64**, 064412 (2001).
[17] S.R. White and D.J. Scalapino, Phys. Rev. Lett. **80**, 1272 (1998).
[18] J. Bonca, J.E. Gubernatis, M. Guerrero, E. Jeckelmann, and S.R. White, Phys. Rev. B **61**, 3251 (2000).
[19] G. Fano, F. Ortolani, and A. Parola, Phys. Rev. B **42**, R6877 (1990).
[20] S. Kneer, Diploma thesis, Universität Würzburg, 1997; R.M. Noack, S. Daul, and S. Kneer, in *Density Matrix Renormalization* (Ref. 3), p. 197.
[21] E. Jeckelmann and S.R. White, Phys. Rev. B **57**, 6376 (1998).
[22] M. Takahashi, *Thermodynamics of One-Dimensional Solvable Models* (Cambridge University Press, Cambridge, 1999), p. 94.
[23] E. Koch and S. Goedecker, Solid State Commun. **119**, 105 (2001).
[24] M. Takahashi, J. Phys. C **10**, 1289 (1977).
[25] W. Metzner and D. Vollhardt, Phys. Rev. B **39**, 4462 (1989).
[26] F.H.L. Essler and A.M. Tsvelik, Phys. Rev. B **65**, 115117 (2002); see also P.W. Wiegmann, Sov. Sci. Rev. Ser. A, **2**, 41 (1980).
[27] F.H.L. Essler (private communication).
[28] S. Lukyanov and A.B. Zamolodchikov, Nucl. Phys. B **607**, 437 (2001).
[29] A.A. Ovchinnikov, Sov. Phys. JETP **30**, 1160 (1970).
[30] F.D.M. Haldane, Phys. Rev. Lett. **60**, 635 (1988); B.S. Shastry, *ibid.* **60**, 639 (1988).
[31] F. Gebhard and D. Vollhardt, Phys. Rev. Lett. **59**, 1472 (1987); Phys. Rev. B **38**, 6911 (1988).
[32] W. Metzner and D. Vollhardt, Phys. Rev. Lett. **59**, 121 (1987); Phys. Rev. B **37**, 7382 (1988).